Role of Oxygen Vacancies on Ferromagnetism in Oxide Dilute Magnetic Semiconductors (CeO_2/TiO_2)

by

Md. Abdullah Al Mamun

Student ID: 0417172002

This thesis paper is submitted in partial fulfillment of the requirements for the degree of

MASTER OF SCIENCE

in

Glass and Ceramic Engineering

Department of Glass and Ceramic Engineering

BANGLADESH UNIVERSITY OF ENGINEERING AND TECHNOLOGY

Dhaka-1000, Bangladesh

February 12, 2020

CANDIDATE'S DECLARATION

IT IS HEREBY DECLARED THAT THIS THESIS PAPER OR ANY PART OF IT HAS NOT BEEN SUBMITTED ANYWHERE ELSE FOR THE AWARD OF ANY DEGREE

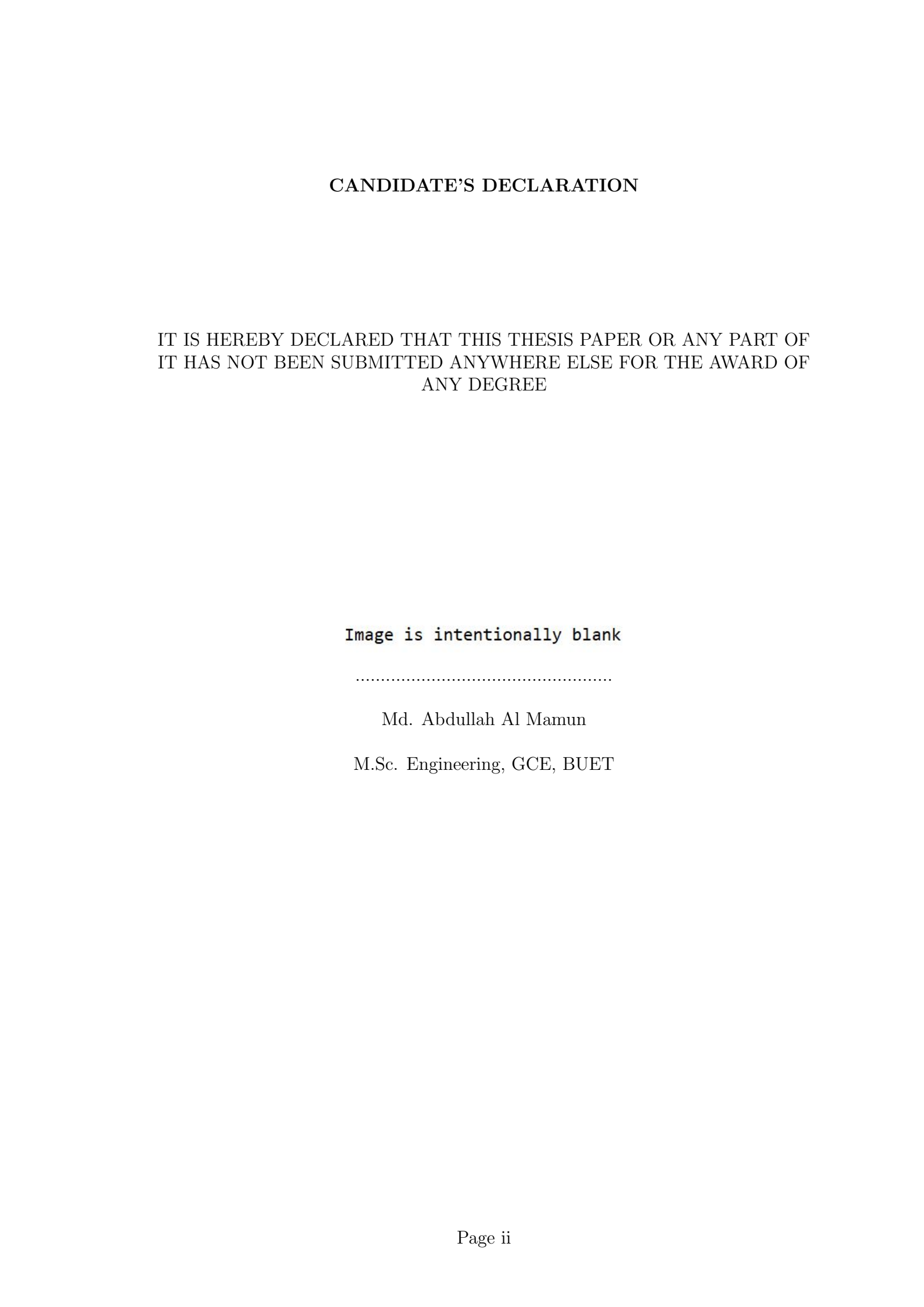

.....

Md. Abdullah Al Mamun

M.Sc. Engineering, GCE, BUET

The thesis titled "Role of Oxygen Vacancies on Ferromagnetism in Oxide Dilute Magnetic Semiconductors: (CeO_2/TiO_2)" submitted by Md. Abdullah Al Mamun, Student No. 0417172002, Session April 2017, has been accepted as satisfactory in partial fulfillment of the requirements for the degree of Master of Science in Glass and Ceramic Engineering on February 12, 2020.

Board of Examiners

.....
Chairman
Dr. Md. Fakhrul Islam
Professor & Head, Dept. of Glass & Ceramic Engineering, BUET, Dhaka-1000

.....
Head
Member (Ex-Officio)
Dept. of Glass & Ceramic Engineering, BUET, Dhaka-1000

.....
Member
Dr. Md. Abdullah Zubair
Assistant Professor, Dept. of Glass & Ceramic Engineering, BUET, Dhaka-1000

.....
Member
Dr. Muhammad Hasanuzzaman
Assistant Professor, Dept. of Glass & Ceramic Engineering, BUET, Dhaka-1000

.....
Member (External)
Dr. Md. Rezwan Khan
Professor and Director, Institute of Engineering & Scientific Research (IESR)
Dept. of Electrical & Electronic Engineering, United International University (UIU), Dhaka-1212

To Almighty Allah

&

To my beloved parents and family

ACKNOWLEDGEMENTS

In the Name of Allah, the Most Gracious and the Most Merciful

Alhamdulillah, all praises to Almighty Allah for the strengths and His blessing in completing this thesis. I would like to thank my supervisor **Dr. Md. Fakhrul Islam** for giving me the opportunity to work in the department of Glass and Ceramic Engineering at BUET. There are not enough words for expressing my sincere gratitude for his willingness to share his knowledge with me through numerous discussions and support since the time of my coursework to completion this degree.

I am immensely grateful to **Dr. A. K. M. Abdul Hakim** for his interest in my work, and encouragement and insight through these years. It was his guidance and support that helped me through all the difficult time. I will surely benefit from his creative thoughts, suggestions and dedication throughout the rest of my life. The same gratitude goes to **Dr. M. A. Matin** for his kind help and support on my research and my life during the past two years.

I also want to thank **Dr. Md. Abdullah Zubair** for thoughtful discussions and sharing his knowledge which inspired me to become a perfectionist researcher in coming years. I would like to express a special word of thanks to my teachers **Dr. Muhammad Hasanuzzaman, Arman Hussain** & **Mehedi Hasan Rizvi** for their continuous support and inspiration during my M.Sc. study.

My warmest thanks go to **Dr. S. A. M. Tofail** from University of Limerick, Ireland for giving his valuable time and thoughts for my thesis work including the state of the art laboratory facilities to characterize my samples. I would like to express my gratitude to **Dr. Vasily Lebedev** and **Dr. Karrina McNamara** at University of Limerick, Ireland for carrying out the TEM and XPS measurements of my samples. I also want to thank **Dr. Sheikh Manjura Hoque**, Chief Scientific Officer and Head, Materials Science Division, Atomic Energy Centre, Bangladesh Atomic Energy Commission, for her support with the magnetic characterization facilities.

I would like to convey my heartiest regards to all of the faculty members, technical and official staff of Department of Glass and Ceramic Engineering at BUET for their assistance and cooperation during this whole time.

Finally, I want to thank my beloved parents and my wife **Manifa Noor** for being there for me. Without their love, understanding and encouragement, this work would be close to impossible to finish.

ABSTRACTS

The fascinating concept of substituting the cation of oxide based dilute magnetic semiconductors (DMS) with transition/rare earth metal ions shows tremendous prospects because of their usefulness in ultrafast spin-charge transport phenomena and their applications. The aim of this thesis is focused on studying the effects of Sm^{3+} substitution for Ti^{4+} ion in TiO_2 lattice from 0 mol% to as high as 20 mol%. Both X-Ray diffraction and electron diffraction analysis show that the substitution of Sm inhibited the grain growth and phase transition from Anatase to Rutile. The particle size distribution estimated from Transmission Electron Microscopy (TEM) shows that particle size was reduced from 53($\pm$10) nm to 10($\pm$3) nm due to addition of Sm content. The photoluminescence and UV-Vis-NIR spectroscopy suggest that all samples exhibit indirect bandgap and addition of Sm content reduces the bandgap because of the presence of shallow trap centers created by oxygen vacancies just below the conduction band. The magnetization vs. applied field (M-H) exhibit dilute ferromagnetic behavior at 300 K for all samples while an evolution of paramagnetic response along with ferromagnetic behavior was noticed with increasing Sm content at 5 K which might be attributed to the presence of the amorphous samarium oxide. Such promising results suggest that the role of oxygen vacancies in formation of amorphous second phase of bulk dopants which might contribute to the net ferromagnetic behavior of dilute magnetic semiconductors (DMS) are worthy of further investigation.

Contents

1 Introduction **1**
- 1.1 Background of the research 1
- 1.2 Dilute Magnetic Semiconductors (DMS) 2
- 1.3 Current challenges in DMS research 4
- 1.4 Objective of this research 4
- 1.5 Thesis overview 5

2 Literature Review **6**
- 2.1 X-ray Absorption Spectroscopy 6
- 2.2 X-ray Magnetic Circular Dichroism 7
- 2.3 Angle Resolved Photoemission Spectroscopy 8
- 2.4 Recent advances in DMS research 9
- 2.5 Origin of ferromagnetism in DMS 14
- 2.6 Role of oxygen vacancy in oxide based DMS 16
- 2.7 Prospects of TiO_2 as DMS 17

3 Conclusions **20**

4 Suggestions for future work **22**

List of Figures

1.1 (a-c) Difference between ferromagnetic material, non-ferromagnetic material and dilute magnetic semiconductor. (d-i) Density of states of different types of semiconductor, ideal half metal and half-metallic semiconductors 3

2.1 Schematic principle of X-ray absorption spectroscopy. (images are taken from the webpage of SLAC, Stanford University) 6
2.2 Difference in 3d orbital due to crystal field splitting in Fe^{3+} 7
2.3 (a)Schematic principle of X-ray magnetic circular dichroism (XMCD) (b) Difference between XAS and XMCD principle [20] 8
2.4 Schematic diagram of angle resolved photoemission spectroscopy . . . 8
2.5 (a) Magnetic-field vs. Hall resistivity ρ_{Hall} and resistivity ρ of $Ga_{(1-x)}Mn_xAs$ vs. temperature. Mn concentration is x=0.053. The change of spontaneous magnetization M_s with temperature is showed in inset [4] (b) X-ray absorption and X-ray magnetic circular dichroism spectra of $Ga_{0.98}Mn_{0.02}As$ [22] 9
2.6 (a) Magnetization vs. temperature of as-implanted and laser annealed (A and B) $In_{0.95}Mn_{0.05}P$ samples (b) XAS and XMCD study of $In_{0.95}Mn_{0.05}P$ [23] 10
2.7 Experimental observation of half-metallic behavior in $Ga_{0.97}Mn_{0.03}As$ by Hard X-ray angle resolved photoemission spectroscopy [25] 10
2.8 Experimental observation of half-metallic behavior in $Ga_{0.975}Mn_{0.025}As$ by soft X-ray angle resolved photoemission spectroscopy [26] 11
2.9 (a) Bound magnetic polaron controlling the ferromagnetism in $Ga_{0.975}Mn_{0.025}As$. (b) Schematic image of magnetic interaction in $Ga_{0.975}Mn_{0.025}As$ crystal structure [26] 11
2.10 Magnetization vs. applied field in $Zn_{(1-x)}Cr_xTe$ [29] 12
2.11 (a) Magnetization vs. applied field (b) Magnetization vs. temperature graph of $Ti_{0.93}Co_{0.07}O_2$ sample [9] 12
2.12 Intrinsic ferromagnetism in transition metal doped TiO_2 thin films . . 13
2.13 (a) Magnetization vs. applied field (b) XAS and (c) XMCD spectra of $Ti_{0.95}Co_{0.05}O_2$ thin film [39] 13
2.14 Bright field STEM image of $Ti_{0.90}Co_{0.10}O_2$ grown on LaAlO_3 substrate. The HAADF and EDX images show the homogeneous doping of Cobalt in TiO_2 [38] 13
2.15 Magnetization vs. applied field in $Ti_{(1-x)}Co_xO_2$ nanoparticles [49] . . 14
2.16 Dilute ferromagnetism observed in undoped non-magnetic oxides due to oxygen vacancies [14] 15
2.17 RKKY type exchange interaction of frustrated spins in $CePO_4$ [50] . 15

2.18 Role of oxygen vacancies in CeO_2 [59] 17
2.19 Crystal Structure of three polymorphs of TiO_2 ($\alpha = \beta = \gamma = 90^\circ$ for all polymorphs) 18
2.20 Difference in bond length and bond angles in rutile and anatase TiO_2 19

CHAPTER 1

INTRODUCTION

1.1 Background of the research

Modern technology stands on the shoulder of semiconductor materials for their immensely useful adaptabilities of physical properties specially the electrical conductivity with an applied electrical field. Despite of having superior conductivity, metals have been outcast by the uniqueness of semiconductor materials in controlling the flow of current. For example, in order to perform a logic function, the ability to distinguish between one and zero is necessary. Semiconductor materials have the capability to transform from insulating to conducting with the help of very small amount of voltage known as gate voltage. When the gate voltage is above a certain level, current flows through a small channel between source and drain; making the material conductive. Again, this flow of current is interrupted when gate voltage is below the level. This directional flow of current in semiconductor is basically driven by very dilute concentration of dopants into a host semiconductor (i.e. 10^{13} to 10^{18} dopant atoms/cm^3 in Si as host material which contains 5×10^{22} atoms/cm^3). By inducing such excess or shortage of electrons via doping, variable electrical resistance can be achieved which makes semiconductor materials useful for switching, amplification or energy conversion applications. This class of semiconductor is known as Transistor and they led the most important paradigm shift in technology by miniturization of devices which in turns reduces the energy utilization by thousand folds. The placement of these transistors on the integrated circuit (IC) is important because the more miniaturized dense IC could be made, the less heat loss would happen which eventually will raise the speed of information process. In 1965, Gordon Moore, one of the cofounder of Intel, predicted that the number of transistors placed on an IC will double in every two years. Companies like Intel, Samsung and NVidia are now fabricating transistors less than 20 nm in size at mass scale and NVidia's new graphics card GF100 is an example of how dense miniaturized a device can become which contains more than 3 Billion transistors. But, this miniaturization to speed up the information process has now reached its saturation limit since it is almost at the edge of atomic scale. On the other side, we are producing more than 2.5 quintillion bytes of data everyday according to Forbes. With days passing by, we are becoming fonder of online based social and financial activities. The energy required for processing this large amount of data is causing global warming at an increased alarming rate. As, the miniaturization of device can no longer provide benefits to us in energy conservation via faster communication, we now must have to think otherwise.

In electronics, only the charge of the electron is utilized while it's another degree of freedom "Spin" remains less remembered. If the spin states can be incorporated with electronic charge to store and process information, the communication will increase by many folds which has been a fascination for decades. Spintronics, an

acronym for SPIN TRansport electrONICS, is one of such promising areas which brought us the novel concept of utilizing both the charge and spin of the electrons. Apart from the formerly known classical states of electron's spinning i.e. rotating clockwise or anticlockwise, there are infinite number of spin states that an electron can possess according to quantum mechanics. If these spin states could be controlled like the current flow in transistor, we would have more options beside the conventional switching technique i.e. current off(0) or on(1). That being said, the electrons carry the spin state must be non-volatile as well as spin polarized and the ferromagnetism needs to be capable of gating. For example, Kreutz *et al.* showed that an organic monolayer, deposited on surface, can provide electrons to compensate the hole carriers of GaMnAs which restrain the ferromagnetism ($T_C < 170K$) [1]. The control over ferromagnetism by changing carrier concentration like Kreutz's research is what we want to achieve at room temperature.

Initially, spin injection attempts were limited to the heterostructure comprising a metallic ferromagnet on semiconductor device [2,3]. But due to serious deficiency of spin injection at metal-semiconductor interface, this idea was replaced by a quest for the ferromagnetism in semiconductor. The concept of ferromagnetic semiconductor was initiated by introducing dilute concentration of magnetic dopants (Mn^{2+}) into a semiconductor material, $Ga_{(1-x)}Mn_xAs$ ($x = 0.015$–0.071) [4]. The ferromagnetism observed in such non-magnetic semiconductors are supposed to be carrier mediated. The excess electrons provided by the dopants delocalize near the fermi level. For certain cases, these delocalized impurity bands become spin polarized and tend to show half-metallic behavior. The materials showed such property were started to be termed as "Dilute Magnetic Semiconductor (DMS)". In an ideal DMS, the charge carriers are spin polarized and behave like half-metallic which enable the charge carriers to be transported by inducing very small applied electrical or magnetic field. By showing high promises of carrier mediated spin-charge transport, DMS materials have raised a lot of enthusiasm in scientific community in the recent years to extend the established CMOS (Complementary Metal Oxide Semiconductor) based electronics towards spintronics devices.

1.2 Dilute Magnetic Semiconductors (DMS)

Dilute magnetic semiconductors are actually non – magnetic materials containing very small amounts of magnetic ions as dopants. Due to these magnetic dopants, the non – magnetic materials show dilute ferromagnetism. But the basic difference between DMS and other ferromagnetic materials is DMS's half metallic behavior which alone controls the spin-charge transport in these materials. Hence, it is noteworthy to revisit the concept of spin polarization and half metallic behavior before going further about DMS.

Spin polarization can be expressed as the ratio of the density of states of up-spin and down-spin electrons at fermi level. The degree of polarization is $P = \frac{N_{up}-N_{down}}{N_{up}+N_{down}}$ where up-spin (N_{up}) and down-spin (N_{down}) electrons denote the electrons polarized in opposite directions. In paramagnetic materials, the degree of polarization is 0 and in conventional ferromagnetic materials the value is between 0 and 1. Only

for the cases of half-metal, the degree of polarization is 1. The schematic density of states of an ideal half metal is given in Fig 1(g). In an ideal half-metal, for specific polarized electrons (either N_{up} or N_{down}) will have density of states in fermi level which does not have any gap between conduction and valence band. For other set of polarized electrons, there will be no density of states in fermi level just like an intrinsic semiconductor. This means that all electrons at fermi level in half-metal are completely polarized and for the presence of gapless density of states at fermi level, the polarized electrons will behave like free electrons of metal. For this reason, these materials are called as half-metal. The concept of half-metal was first predicted by Groot *et al.* during the electronic band structure calculation of NiMnSb and PtMnSb [5]. Coey *et al.* explained the half metallic behavior in CrO_2 and predicted that the half-metallicity in semiconductors can be classified in two types as showed in Fig 1 (h) & (i) [6].

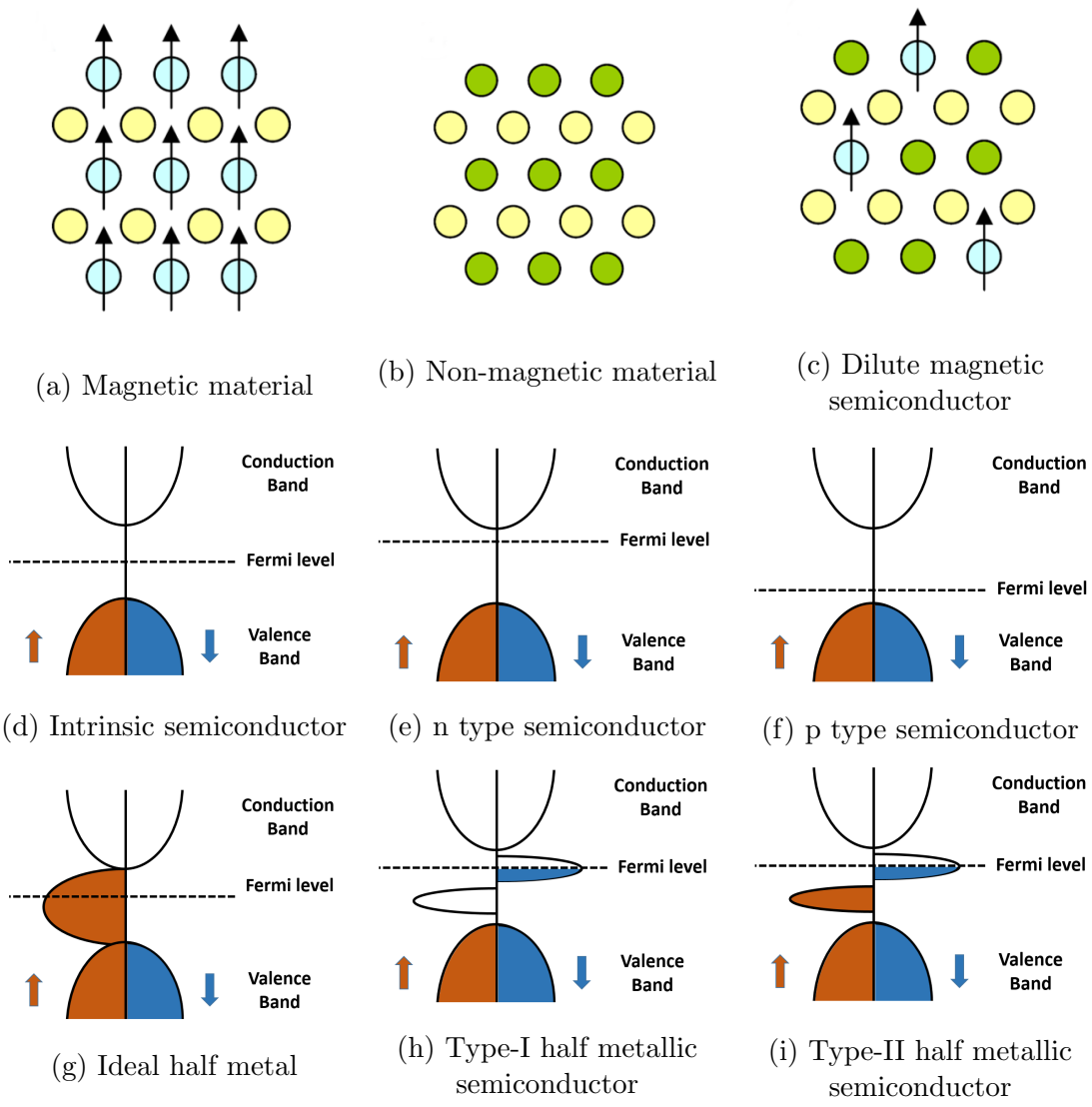

(a) Magnetic material (b) Non-magnetic material (c) Dilute magnetic semiconductor

(d) Intrinsic semiconductor (e) n type semiconductor (f) p type semiconductor

(g) Ideal half metal (h) Type-I half metallic semiconductor (i) Type-II half metallic semiconductor

Figure 1.1: (a-c) Difference between ferromagnetic material, non-ferromagnetic material and dilute magnetic semiconductor. (d-i) Density of states of different types of semiconductor, ideal half metal and half-metallic semiconductors

The bands at fermi level are originated from the delocalized d or f orbital electrons in both types of half-metallic semiconductors. From Fig 1 (h) & (i), it can be clearly understood that the bands in type I material are comprised of less than half filled d or f orbital electrons while in type II, the bands are comprised of more than half-filled d or f orbital electrons. Although the density of states of half-metallic semiconductor deviate from the gapless states of half-metals, the spin polarized delocalized electrons can be transported by hopping from one site to another [6].

In dilute magnetic semiconductor, the magnetic dopants have excess electrons which delocalize at fermi level. It is noteworthy to mention that the dilute magnetic semiconductors should have non-zero spin polarization to achieve half-metallicity. If the half-metallic behavior can be made stable at room temperature, only then the DMS materials will be able to bring a paradigm shift in technology by integrated in logic devices, spin polarized light emitting diodes, non – volatile memory storages, spin field effect transistors etc.

1.3 Current challenges in DMS research

The earliest discovery of dilute magnetic semiconductors were reported for Mn doped II-IV and III-V alloys. In 1988, Furdyna *et al.* studied the physical properties of $Cd_{(1-x)}Mn_xSe$ and $Hg_{(1-x)}Mn_xTe$ but the curie temperature was around 40 K [7]. In 1989, Munekata *et al.* observed the properties of dilute magnetic semiconductor in $Ga_{(1-x)}Mn_xAs$ while the curie temperature was around 100 K [8]. Since then half metallic behavior in these materials specially in $Ga_{(1-x)}Mn_xAs$ was deliberately studied but the curie temperature could not be raised above 170 K. The quest for a room temperature DMS got a new dimension when Matsumoto *et al.* reported extrinsic ferromagnetism in $Ti_{(1-x)}Co_xO_2$ which has very high curie temperature (600 K) [9]. To this day, dilute ferromagnetism at room temperature has been observed in non-magnetic oxides like ZnO, In_2O_3, CeO_2, SnO_2, CuO_2 etc [10–13]. But the concept of making DMS by doping of magnetic impurities was changed when room temperature ferromagnetism was observed in undoped non-magnetic oxides. Besides, magnetic clusters and secondary phases have been found to contribute to extrinsic ferromagnetism in these oxides [14–16]. Therefore, creation of any spintronics device based on these oxide based DMS materials remains halted due to the true understanding of the origin of ferromagnetism in these materials.

1.4 Objective of this research

The aim of this research is focused on the dilute ferromagnetism in $Ti_{(1-x)}Sm_xO_2$ ($0 \leq x \leq 0.2$) nanoparticles. Among the wide bandgap semiconductors, TiO_2 is the most extensively studied material for its superior chemical stability and high curie temperature. The primary reason for Sm^{3+} substitution in TiO_2 is to create oxygen vacancy. The electronic configuration of Sm and Ti are [Xe] $4f^6$ $6s^2$ and [Ar] $3d^2$ $4s^2$ respectively. But the preference of Sm^{3+} (Sm^{3+}=[Xe] $4f^5$) substitution stems from the fact that it has odd number of excess electrons when it substitutes Ti^{4+} in TiO_2. The number of excess electrons is important because they are supposed to be delocalized and induced non-zero spin polarization at fermi level. The delocalized electrons tend to pair themselves by crystal field splitting for energy minimization.

For example, Fe^{2+} ([Ar] $3d^6$) has four unpaired d oribital electrons but after crystal field splitting Fe^{2+} tends to have 3 pairs of d electrons which in turns yield near to zero spin polarization. On another case, Fe^{3+} ([Ar] $3d^5$) five unpaired electrons in valence band. Because having odd number of electrons, it is impossible to nullify the net spin polarization of Fe^{3+} by electron's ownselves pairing mechanism. However, in this research Sm^{3+} was chosen for its odd numbers of f orbital electrons in valence band which are supposed to exhibit strong spin-orbit interaction.

Another reason of Sm^{3+} substitution in TiO_2 is its larger ionic radius (Sm^{3+}=1.08 $\mathring{A}$ and Ti^{4+}=0.68 $\mathring{A}$). One of the main goals of this research is to investigate what happens beyond the solid solubility limit of Sm^{3+} substitution. As it is previously stated that there are discrepancies on the origin of ferromagnetism in oxide DMS materials which mostly revolve around the nature of substitution. Hence it is crucial to investigate the structural purity beyond solid solubility limit of substitution such as the formation & growth of the interface of any 2nd phase and their effect on optical and magnetic properties. So, the aim of this research can be summarized as:

- To study the effect of Sm^{3+} substitution on the structural, optical and magnetic properties of TiO_2
- To investigate the nature of formation and growth of any second phase beyond solid solubility limit of substitution

1.5 Thesis overview

Chapter 2 starts with a brief review on recent progress in dilute magnetic semiconductors and the experimental techniques to investigate the spin polarization in these materials. It will also discuss several theoretical models on the origin of ferromagnetism in DMS. Finally there will be a brief review on recent theoretical and experimental research on TiO_2. Chapter 3 describes the experimental methodology and introduces the detailed synthesis process followed by the structural, morphology, optical and magnetic characterization techniques. Chapter 4 discusses the results obtained from experiments and how they support an elucidation of this research which is concisely given in Chapter 5.

CHAPTER 2

LITERATURE REVIEW

The requirement of dilute magnetic semiconductor is its non-volatile ferromagnetism which must have non-zero spin polarization at fermi level. To this day, extensive research have been performed on dilute magnetic semiconductors. During exploitation the prospects of DMS in any material a number of questions must be carefully resolved. The primary questions are definitely about the structural purity of the sample such as any presence of 2nd phase in X-ray and electron diffraction study, any presence of metallic cluster of dopants in X-ray photoelectron study, any presence of satellite peaks due to oxygen vacancies in the valence band spectra etc. If these questions are resolved then next questions will come forward which are about the spin polarization nature. Before going further on the spin polarization in DMS, it is required to revisit the concepts of three fascinating photoemission spectroscopy techniques which are X-ray absorption spectroscopy (XAS), X-ray magnetic circular dichroism (XMCD) and angle resolved X-ray photoelectron spectroscopy (ARPES). This chapter begins with a plain explanation of these powerful spectroscopy techniques.

2.1 X-ray Absorption Spectroscopy

X-ray absorption spectroscopy provides a clear picture of valence shell by exciting a core level electron to an empty valence shell. In magnetic materials, the valence shell is typically 3d or 4f and they are partially filled. The excited photoelectrons take position in the empty places in d or f orbitals and eventually return to ground state by emitting a fluroscent/auger electrons. The detector in XAS capture and analyze the auger electrons. Peaks are splitted due to spin-orbit interaction of core level electrons.

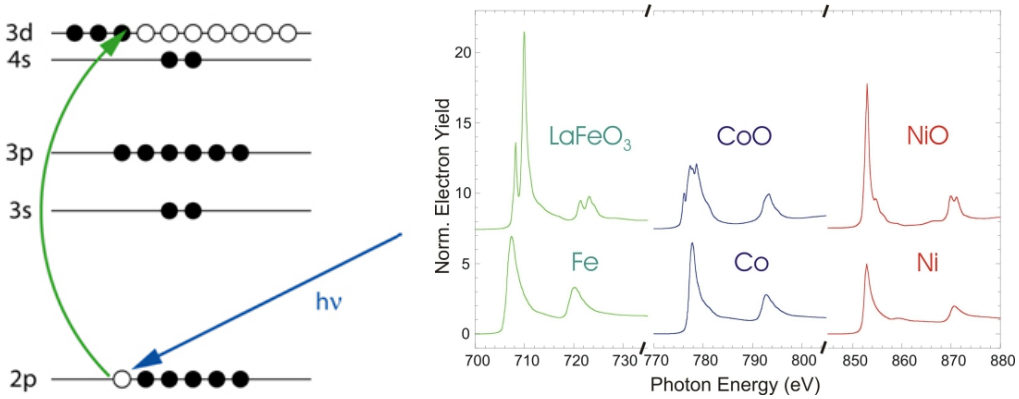

(a) Excitation of a core level electron to valence shell

(b) Difference of X-ray absorption in metal and oxide

Figure 2.1: Schematic principle of X-ray absorption spectroscopy. (images are taken from the webpage of SLAC, Stanford University)

Usually metal shows 2 peaks in XAS while oxides show multiplets as spin-orbit interactions are more localized in oxide materials. Total intensity of the peaks is proportional to the empty d or f orbital density of states. Although XAS can depict the density of states in valence band but it cannot provide any details of spin polarization. For example, the electron configuration of Fe is [Ar] $3d^6$ $4s^2$ and for Fe^{3+} it is [Ar] $3d^5$.

(a) 3d orbital in ground state

(b) crystal field splitting of 3d orbital

Figure 2.2: Difference in 3d orbital due to crystal field splitting in Fe^{3+}

In XAS, the photo-excited core level electrons just fill up the empty states in 3d orbital and there will be no difference in the observed absorption spectra for crystal field splitting. During investigation of spin polarization, observation of only density of states is not enough. For example, XAS cannot differentiate between the density of states for 5 spin-up electrons showed in Fig 2.2(a) and the density of states for 3 spin-up & 2 spin-down electrons showed in Fig 2.2(b). This problem has been resolved by X-ray magnetic circular dichroism spectroscopy.

2.2 X-ray Magnetic Circular Dichroism

X-ray magnetic circular dichroism (XMCD) is a special feature of X-ray absorption spectroscopy (XAS). Dichroism means polarization dependent light absorption of any materials. In simple terms, XMCD is basically an XAS placed in a magnetic field where the incident light is polarized. The left or right circularly polarized photons transfer their angular momentum to the core level electrons. Since change of spin momentum is forbidden in electric dipole transition, the photo-ejected electrons carry the same angular momentum to the valence band. The theory of XMCD was first proposed by Erskine *et al.* in 1986 and the experimental proof of XMCD was demonstrated by Gerrit van der Laan *et al.* in 1986 [17, 18]. A list of synchroton facilities for XMCD around the world is given in the reference [19].

Fig 2.3 shows a schematic mechanism of XMCD. At ground state, 2p electrons of Cobalt metal are usually splitted in $j = \frac{3}{2}$ level (L_3 edge) and $j = \frac{1}{2}$ level (L_2 edge). It is noteworthy to mention that spin and orbit are coupled parallel in L_3 edge and antiparallel in L_2 edge. At first, the right circularly polarized incident light excites the 2p electrons which are parallel to the helicity of the light (spin-up electrons). Similarly the left circularly polarized light excites the antiparallel electrons at 2p core states (spin-down electrons). These electrons carry the angular momentum and fill up the unoccupied empty states in 3d orbital. The net difference of available places for spin-up and spin-down electrons in unoccupied 3d orbitals can be understood by the XMCD graph.

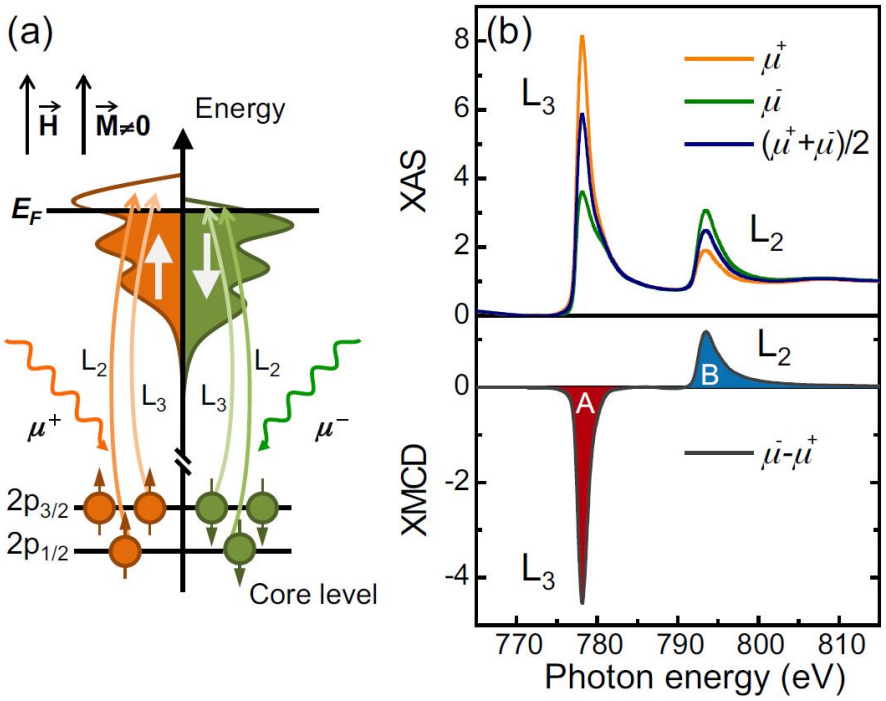

Figure 2.3: (a)Schematic principle of X-ray magnetic circular dichroism (XMCD) (b) Difference between XAS and XMCD principle [20]

2.3 Angle Resolved Photoemission Spectroscopy

Angle resolved photo emission spectroscopy is the characterization technique for direct observation of the electronic band structure of any crystalline material.

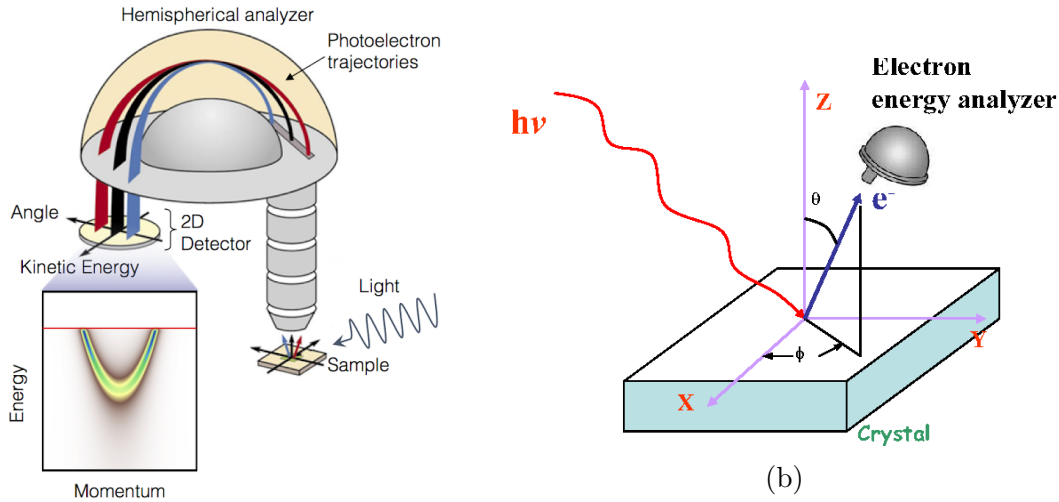

Figure 2.4: Schematic diagram of angle resolved photoemission spectroscopy

Like the other photoemission spectroscopy, ARPES is based on the photoelectric effect which was pioneered by Einstein. When a sample is irradiated by incident

light with sufficient energy, an electron from the surface of the material can absorb the energy of photon and escape the surface. The kinetic energy required for this process is $h\nu - \phi$ ($h\nu$ is the photon energy and ϕ is the work function of the material). ARPES measures the kinetic energy of a photoelectron and calculates its original binding energy using the energy conservation law. Electrons having different momentum will escape from the surface at different angles and hence the momentum resolution of the photoejected electrons can be determined by analyzing the angle of the photoemission.

2.4 Recent advances in DMS research

This section will briefly present a review on recent progress in DMS research. Over last few decades extensive research were performed on DMS properties in III-V, II-VI and oxide materials. The seminal research work by Munekata *et al.* first demonstrated the DMS properties in III-V materials [8]. In their work, they have grown $In_{(1-x)}Mn_xAs$ (x $\leq$ 0.18) on both InAs and GaAs substrates by molecular beam epitaxy. The films showed intrinsic semiconducting behavior (n-type) but the curie temperature was far below room temperature. Hayashi *et al.* found extraordinary magnetoresistance in $Ga_{(1-x)}Mn_xAs$ [21]. The curie temperature and magnetization were increased with Mn concentration. Matsukura *et al.* explained that the ferromagnetism observed in $Ga_{(1-x)}Mn_xAs$ follows Ruderman-Kittel-Kasuya-Yosida (RKKY) exchange interaction [4].

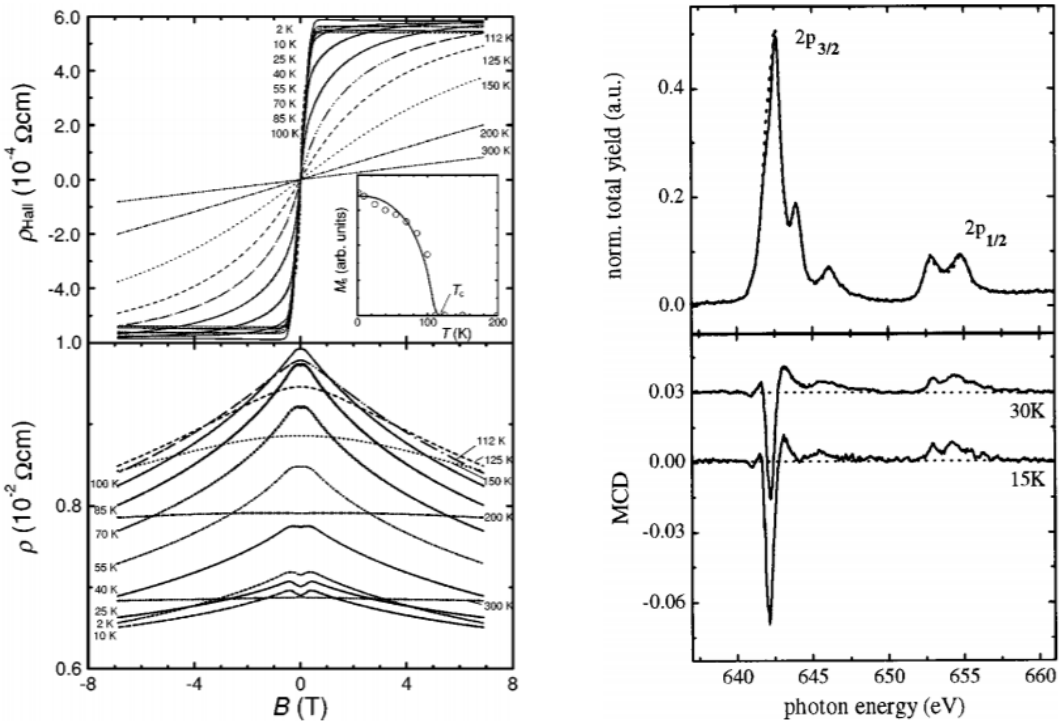

(a) (b)

Figure 2.5: (a) Magnetic-field vs. Hall resistivity ρ_{Hall} and resistivity ρ of $Ga_{(1-x)}Mn_xAs$ vs. temperature. Mn concentration is x=0.053. The change of spontaneous magnetization M_s with temperature is showed in inset [4] (b) X-ray absorption and X-ray magnetic circular dichroism spectra of $Ga_{0.98}Mn_{0.02}As$ [22]

Khalid *et al.* found strong spin polarization at fermi level in $In_{0.95}Mn_{0.05}P$ sample which showed intrinsic semiconducting behavior and negative magnetoresistance [23]. Scarpulla *et al.* reported carrier mediated ferromagnetism in $Ga_{0.94}Mn_{0.06}P$ where strongly localized hole states are created just above the valence band due to Mn doping [24]. But for both $Ga_{(1-x)}Mn_xP$ and $In_{(1-x)}Mn_xP$ the curie temperature remains around 60 K.

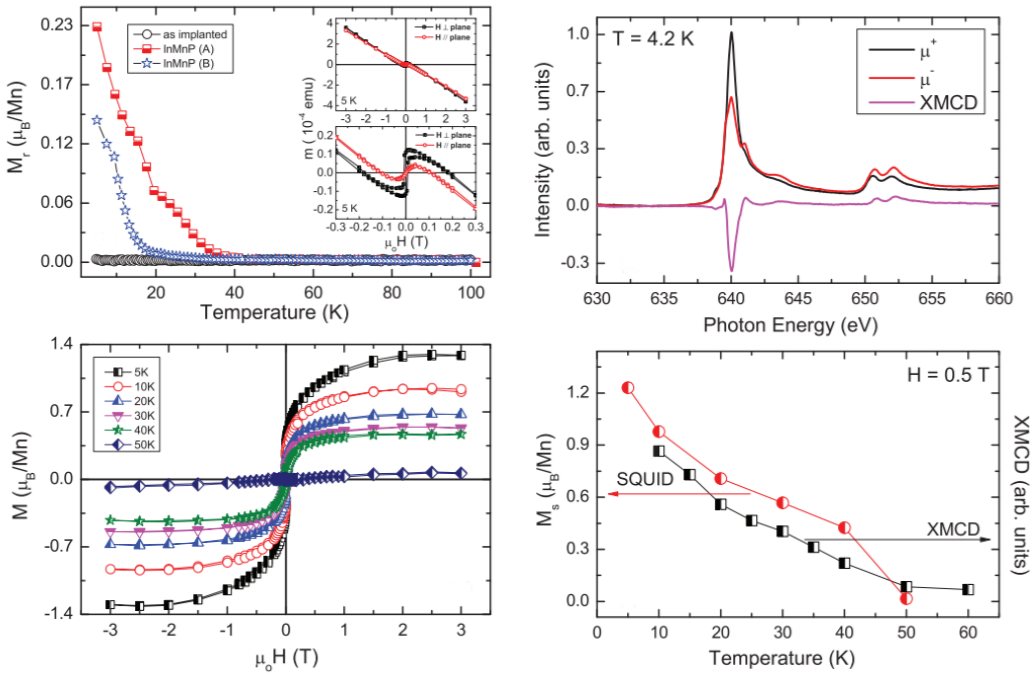

(a) (b)

Figure 2.6: (a) Magnetization vs. temperature of as-implanted and laser annealed (A and B) $In_{0.95}Mn_{0.05}P$ samples (b) XAS and XMCD study of $In_{0.95}Mn_{0.05}P$ [23]

Gray *et al.* experimentally proved the half-metallic behavior of $Ga_{0.97}Mn_{0.03}As$ by analyzing the electronic band structure using Hard X-ray angle resolved photoemission spectroscopy [25]. The Mn induced density of states were observed between fermi level and valence band maxima in their experiment.

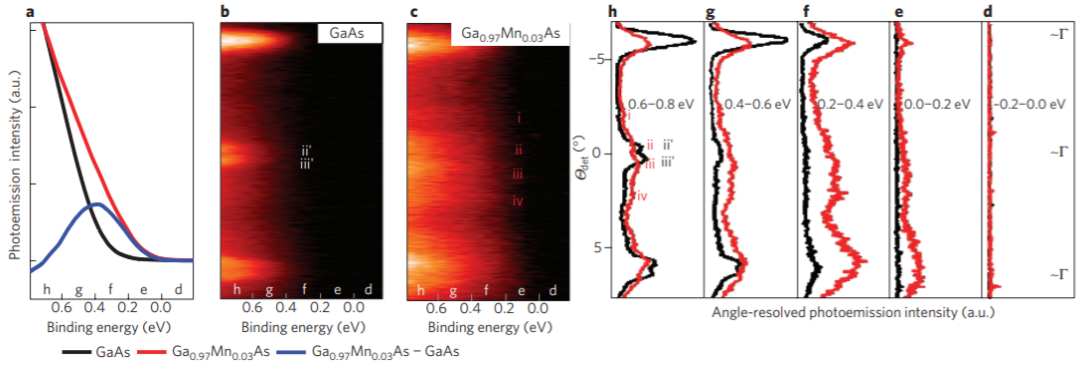

Figure 2.7: Experimental observation of half-metallic behavior in $Ga_{0.97}Mn_{0.03}As$ by Hard X-ray angle resolved photoemission spectroscopy [25]

Kobayashi *et al.* also reported half-metallic behavior of $Ga_{0.975}Mn_{0.025}As$ in

their seminal research paper [26]. Nemvsak *et al.* also reported half-metallic behavior in $Ga_{0.95}Mn_{0.05}As$ by using standing wave angle resolve photoemission spectroscopy (SW-ARPES) [27]. Keqi *et al.* investigated the electronic structure of $Ga_{0.98}Mn_{0.02}P$ by using hard X-ray angle resolved photoemission spectroscopy and observed Mn induced impurity states near valence band maxima [28].

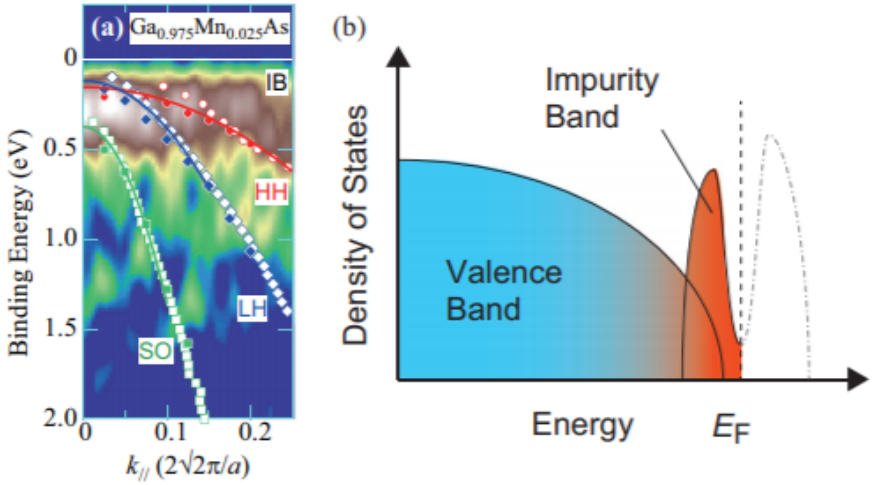

Figure 2.8: Experimental observation of half-metallic behavior in $Ga_{0.975}Mn_{0.025}As$ by soft X-ray angle resolved photoemission spectroscopy [26]

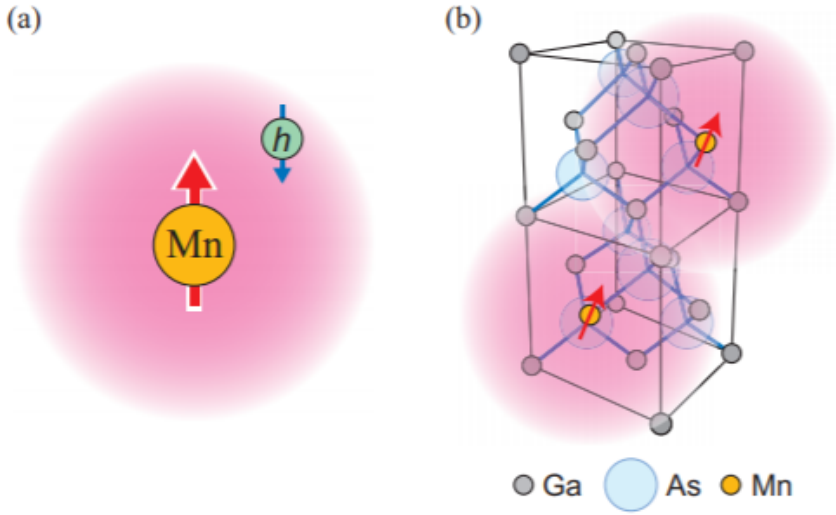

Figure 2.9: (a) Bound magnetic polaron controlling the ferromagnetism in $Ga_{0.975}Mn_{0.025}As$. (b) Schematic image of magnetic interaction in $Ga_{0.975}Mn_{0.025}As$ crystal structure [26]

Furdyna *et al.* first reported II-VI based dilute magnetic semiconductors ($Cd_{(1-x)}Mn_xSe$ and $Hg_{(1-x)}Mn_xTe$) in 1988 [7]. Zhao *et al.* reported short-range magnetic ordering in $Zn_{(1-x)}Cr_xTe$ [29]. Observation of similar short-range ferromagnetic interaction in II-VI based DMS have been reported in many literatures in last few decades [30–32].

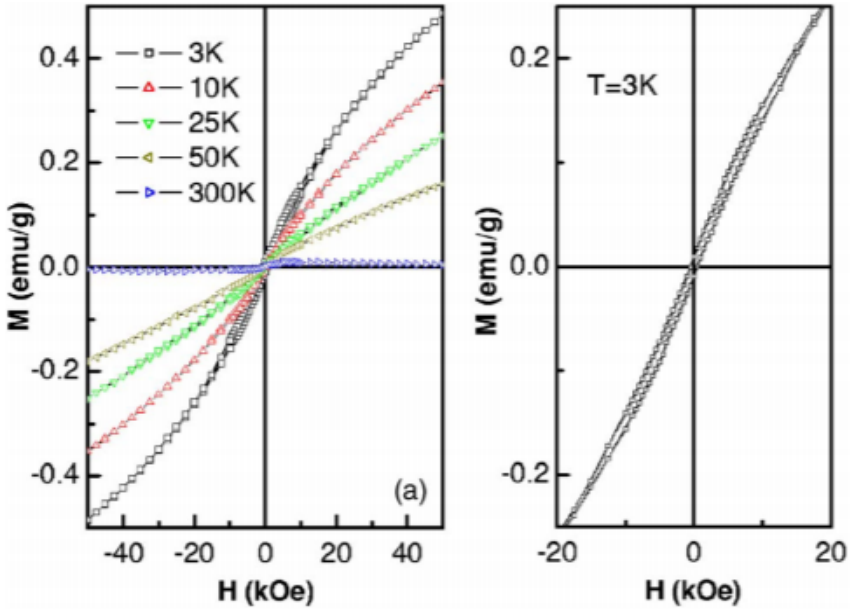

Figure 2.10: Magnetization vs. applied field in $Zn_{(1-x)}Cr_xTe$ [29]

Matsumoto *et al.* first demonstrated the intrinsic ferromagnetism in Co:TiO_2 which showed high curie temperature [9]. This groundbreaking discovery led to extensive research on DMS in oxide based materials since 2001 [33–37]. Yamada *et al.* reported electrically induced ferromagnetism in $Ti_{0.90}Co_{0.10}O_2$ at room temperature [38]. Saadaoui *et al.* reported intrinsic ferromagnetism observed in $Ti_{0.95}Co_{0.05}O_2$ thin film is controlled by oxygen vacancy [39]. Several seminal research works also exhibit intrinsic carrier mediated ferromagnetism in other non-magnetic oxides like ZnO, In_2O_3, CeO_2 [10, 40–46].

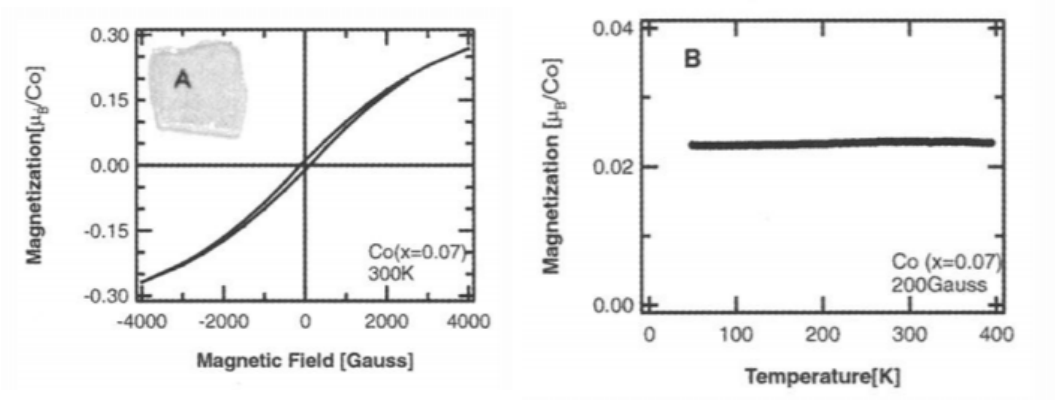

(a) (b)

Figure 2.11: (a) Magnetization vs. applied field (b) Magnetization vs. temperature graph of $Ti_{0.93}Co_{0.07}O_2$ sample [9]

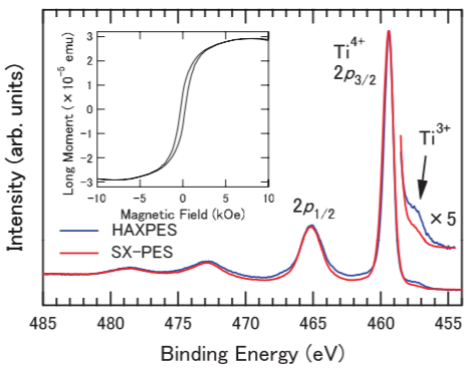

(a) Soft X-ray and Hard X-ray photoemission spectroscopy of $Ti_{0.95}Co_{0.05}O_2$ thin film [47]

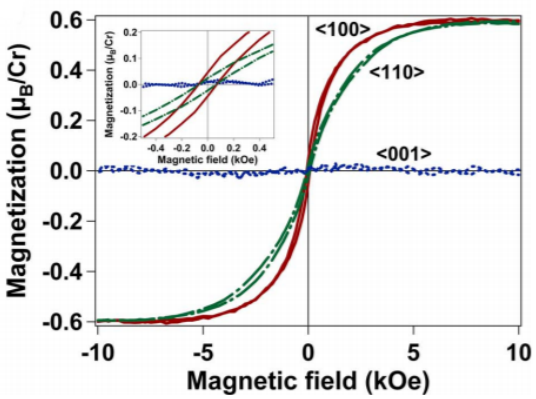

(b) Magnetization vs. applied field in $Ti_{0.91}Co_{0.09}O_2$ thin film [48]

Figure 2.12: Intrinsic ferromagnetism in transition metal doped TiO_2 thin films

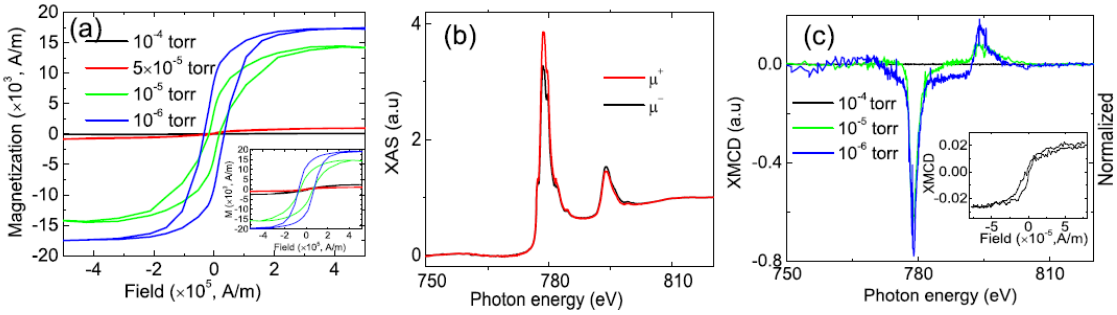

Figure 2.13: (a) Magnetization vs. applied field (b) XAS and (c) XMCD spectra of $Ti_{0.95}Co_{0.05}O_2$ thin film [39]

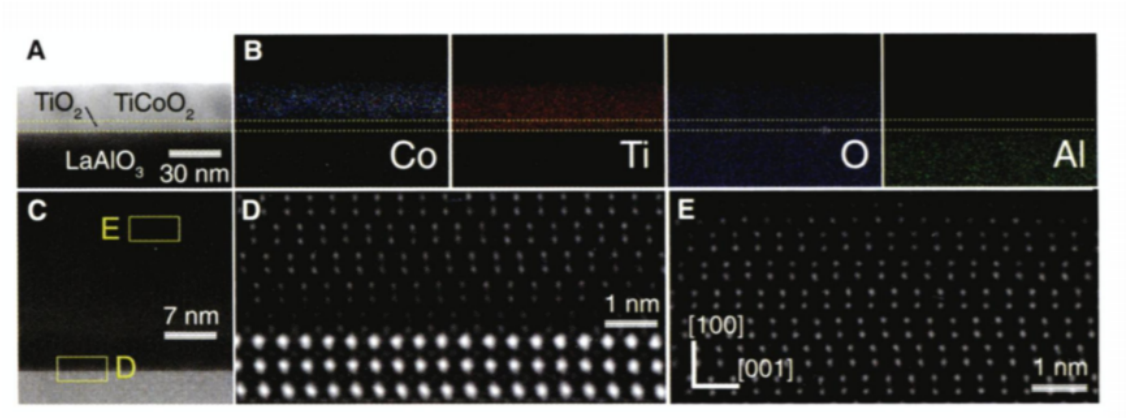

Figure 2.14: Bright field STEM image of $Ti_{0.90}Co_{0.10}O_2$ grown on $LaAlO_3$ substrate. The HAADF and EDX images show the homogeneous doping of Cobalt in TiO_2 [38]

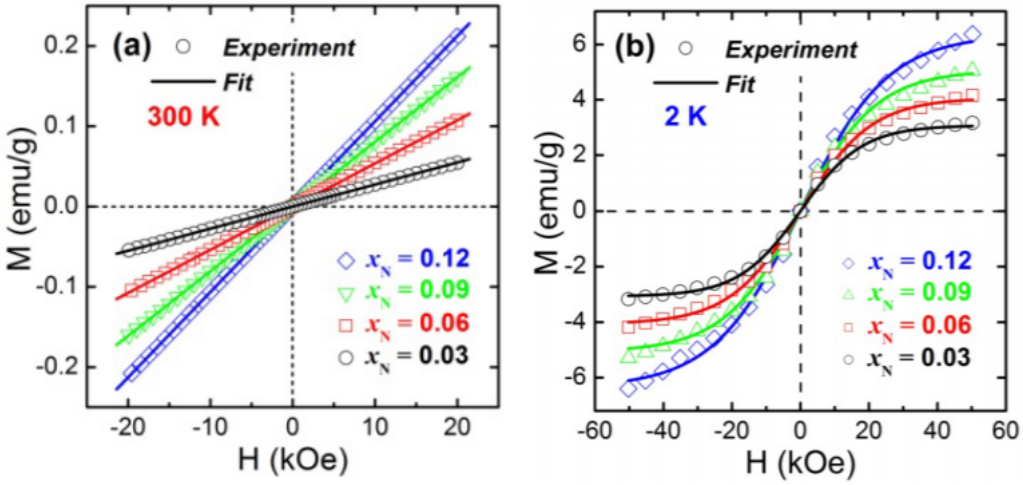

Figure 2.15: Magnetization vs. applied field in $Ti_{(1-x)}Co_xO_2$ nanoparticles [49]

2.5 Origin of ferromagnetism in DMS

Despite extensive research have been performed on DMS over last few decades, the true origin of ferromagnetism remains still unclear. The principle concept of DMS is to induce ferromagnetism by adding magnetic dopants in a non-magnetic semiconductor material. But Sunderasan *et al.* showed that ferromagnetism might be found in non-magnetic materials if their particle size is in nanoscale range [14]. In their research, they found that variation of annealing temperature of undoped non-magnetic oxides like ZnO, In_2O_3, CeO_2 and Al_2O_3 is related to observed dilute ferromagnetism. In explanation they attributed this phenomena to be controlled by the concentration of oxygen vacancies on surface of the nanoparticles. According to Sunderasan *et al.* the surface oxygen vacancies create localized electron spin moments which follow Ruderman-Kittel-Kasuya-Yosida (RKKY) interaction. The RKKY interaction is basically a long range exchange interaction between d or f orbital electrons and it decays in an algebraic manner with respect to the distance between spins. The theory of RKKY type exchange interaction was inspired from mean field Zener model which pioneered the theoretical proof of DMS properties in Mn doped II-VI and III-V semiconductors.

Zener model suggests that delocalized charge carriers enhances the ferromagnetic interaction of localized spins in metallic system. But the exchange interaction in DMS is different than the short range d-d exchange interaction in 3d metal. Applying the mean field theory to the Zener model, it's found that the ferromagnetism in DMS can be well described by the long range p-d exchange interaction between localized and delocalized spins. According to this theory, doped holes redistribute themselves by maintaining favorable delocalization length so that the energy of the system becomes less. The mean field Zener model established an exchange constant (J_{p-d}) which can be experimentally determined. This model not only predicted a number of DMS candidates including zinc blende and wurzite type wide band gap oxides and nitrides but also presented a mechanism to increase curie temperature in those materials. According to the suggestion, cure temperature can be raised by enhancing the hybridization energy which is proportional to a^{-3} (a is the lattice constant).

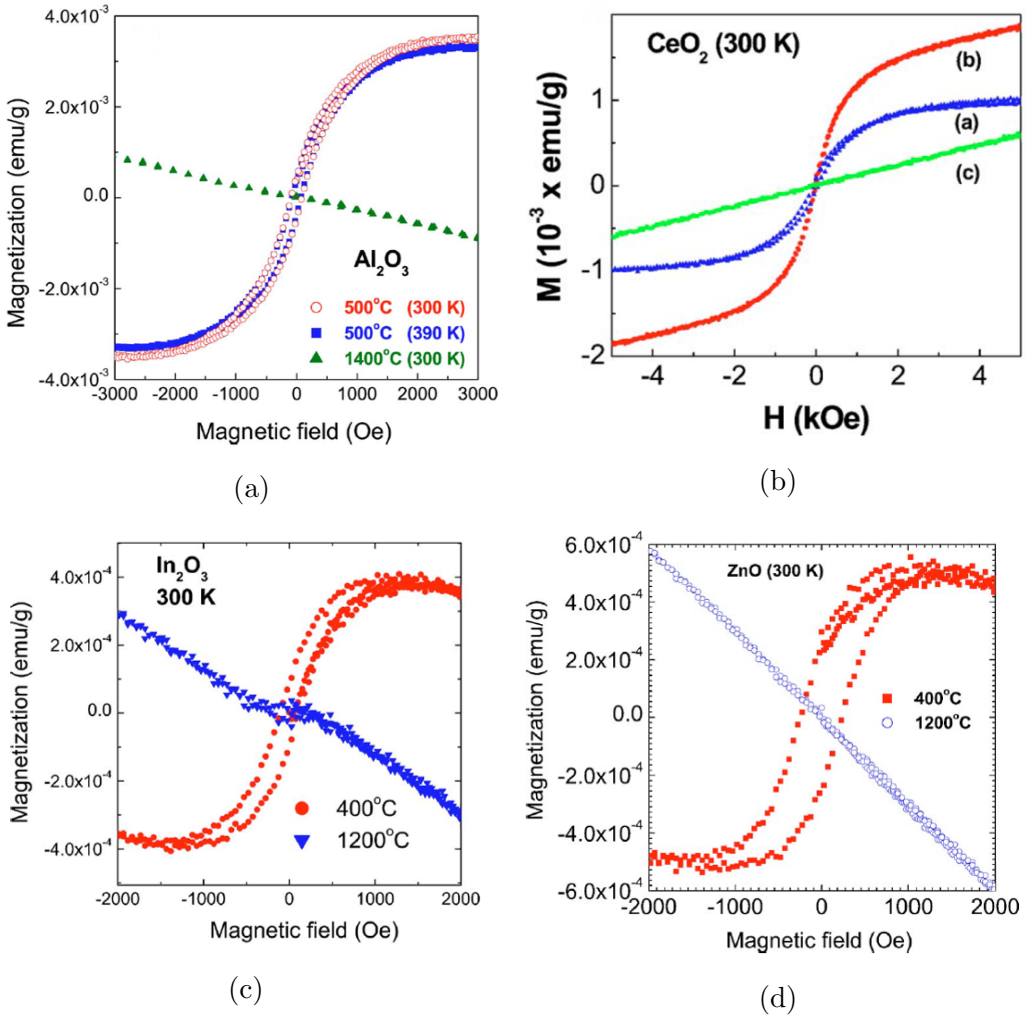

Figure 2.16: Dilute ferromagnetism observed in undoped non-magnetic oxides due to oxygen vacancies [14]

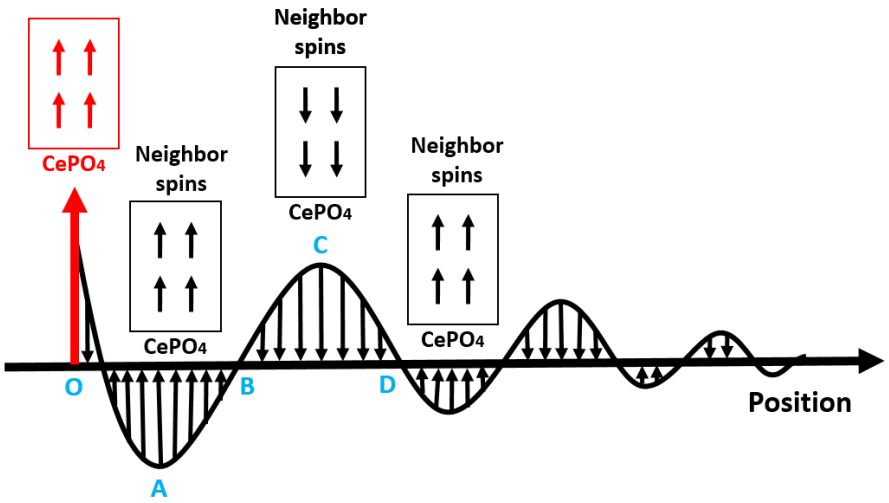

Figure 2.17: RKKY type exchange interaction of frustrated spins in $CePO_4$ [50]

The mean field Zener model predicted p-type DMS candidates where the hole

induced bands will be just above the valence band. This theory was proved wrong when it was found that the predicted DMS candidates showed n-type semiconducting behavior. Actually Zener model considered d orbital electrons will not participate in charge transport and it was based on Mn induced band states. The case is different for other transition metal ions as Mn has a unique orbital levels which is not like the other transition metal ions. However, RKKY interaction resolved the issue which focused on charge carrier mediated interaction in the DMS. The concept of mean field Zener model and RKKY is almost same. RKKY explains the ferromagnetic-antiferromagnetic interaction when the concentration of holes is larger than that of spins which cannot be explained by Zener model.

In contrast to direct and indirect exchange interaction described by mean field Zener model and RKKY model, there are also some additional exchange interaction which have been found non-trivial to explain the ferromagnetism in DMS. Among them the concept of bound magnetic polaron is most relevant. When the delocalized spins act as a cluster and their behavior is controlled by the effective mass of the cluster. The polaronic interaction increases with decrease in temperature. The interaction between the localized polaron is antiferromagnetic. This model has become popular to explain the ferromagnetism observed in a low carrier density DMS. It is noteworthy to mention that none of these theories can alone truly describe the universal nature of the ferromagnetism in DMS.

2.6 Role of oxygen vacancy in oxide based DMS

Oxide based DMS have showed high promises for room temperature intrinsic ferromagnetic behavior but the fundamental limitation is the true understanding of ferromagnetism in these materials. Oxygen vacancies play crucial role in determination of ferromagnetic interaction which have extensively studied by both computational and experimental approaches. In previous section, the research of Sunderasan *et al.* clearly demonstrated the influence of oxygen vacancies on the observed ferromagnetism in undoped non-magnetic oxides. Oxygen vacancy induced band states strongly interact with delocalized electrons and are capable of nullifying the non-zero spin polarization at fermi level. Hence the role of oxygen vacancy has been deliberately studied since the discovery of intrinsic ferromagnetism in $Co : TiO_2$.

Bryan *et al.* showed that the oxygen vacancies at grain boundaries are responsible for the high curie temperature ferromagnetism in Cr and Co doped TiO_2 nanomaterials [51]. Chowdhury *et al.* reported that Mn doping distorts the TiO_2 crystal structure generating oxygen vacancies at surface which reduce the mobility of charge carriers. They attributed the ferromagnetic interaction to be controlled by oxygen vacancies via forming bound magnetic polarons in the system [52]. Such kind of surface oxygen vacancy induced ferromagnetism has been reported for TiO_2, SnO_2, TiO_2 and ZnO in many literatures [53–58].

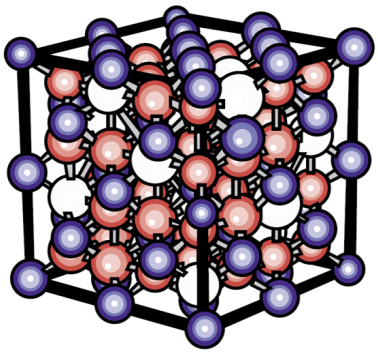

(a) Stoichiometric Crystal Structure of CeO_2-Ce_2O_3. Blue, Red and White spheres indicate Cerium, Oxygen atoms & Oxygen vacancy

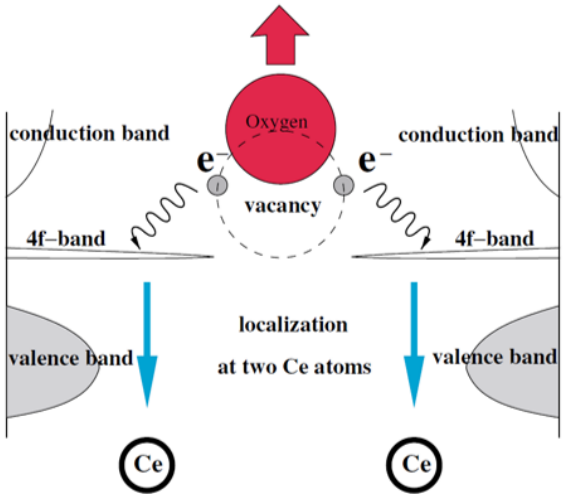

(b) Oxygen vacancy leaves electron to its neighbor two Ce^{4+} and they become Ce^{4+}

Figure 2.18: Role of oxygen vacancies in CeO_2 [59]

2.7 Prospects of TiO_2 as DMS

The groundbreaking discovery of Co:TiO_2 pioneered the quest for a DMS showing intrinsic semiconducting behavior at room temperature. Although, the prospects of DMS have been reported for other non-magnetic oxides like ZnO, In_2O_3 and CeO_2, the superior stability of TiO_2 makes itself a unique candidate for DMS. For example, CeO_2 has almost the similar lattice matching with Si but due to the unstability the DMS prospects in CeO_2 are considered much volatile than the others. The exceptional capability of charge transfer between Ce^{3+} and Ce^{4+} enables CeO_2 as an outstanding material for oxygen storage and catalyst like applications. But this unstability is a serious concern when it comes to any device application. From this perspective, TiO_2 outruns the other oxide DMS candidates.

TiO_2 has three stable polymorphs - anatase, rutile and brookite. Among them rutile is the most stable one in bulk and anastase is most stable in nanoscale range due to less surface energy [60]. Both anatase and rutile have tetragonal crystal structure while the titanium atom is surrounded by six oxygen atoms in an octahedral arrangement. During heat treatment, anatase undergoes a phase transition in the temperature range 600-700 $^{\circ}C$. Although, the bandgap of anatase (3.2 eV) is larger than rutile (3 eV), photoactivity of anatase is greater than the rutile due to anatase's electronic structure and surface morphology.

Transition and rare earth metal doped TiO_2 thin films and nanoparticles have been widely studied. Among them few literatures studied Sm doped TiO_2 nanoparticles and thin films. Xiao *et al.* synthesized $Ti_{(1-x)}Sm_xO_2$ ($0 \leq x \leq 0.015$) via sol-gel autocombustion technique. In their research they investigated the photocatalytic properties of rutile-anatase heterostructure and did not carry out the magnetic characterization [61].

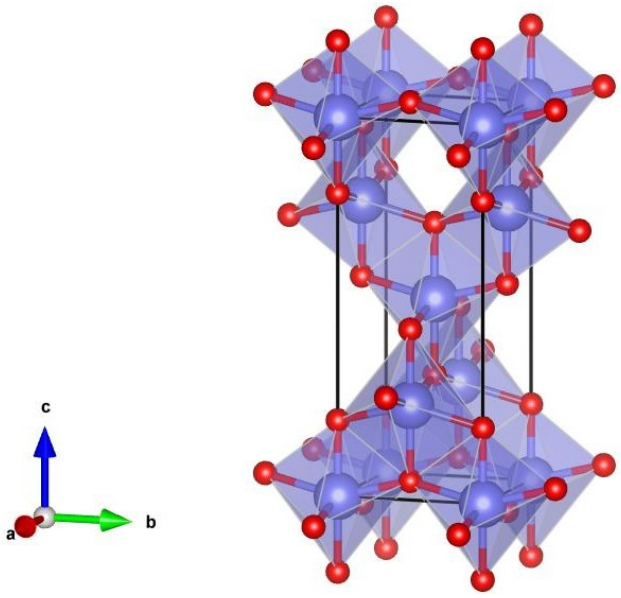

(a) Anatase ($a = b = 3.78\mathring{A}, c = 9.51\mathring{A}$)

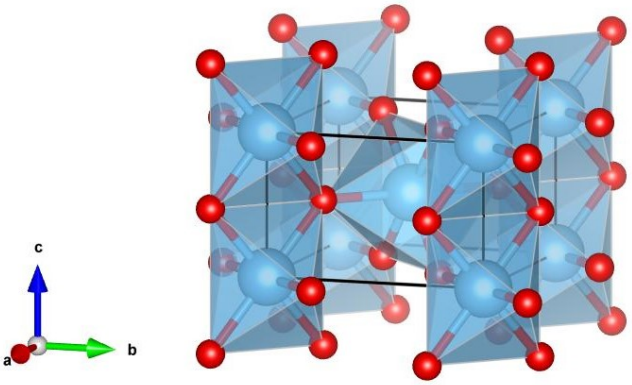

(b) Rutile ($a = b = 4.59\mathring{A}, c = 2.95\mathring{A}$)

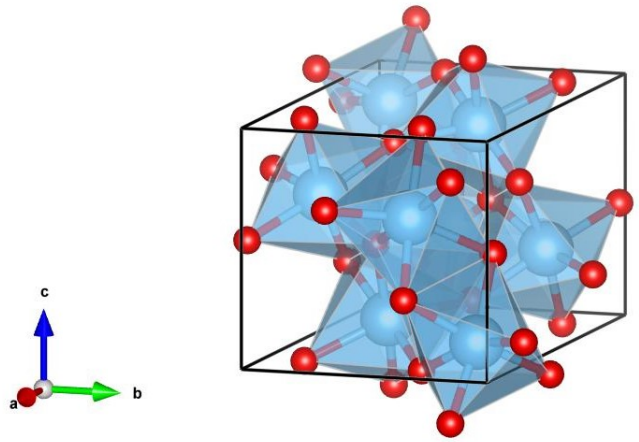

(c) Brookite ($a = 5.45\mathring{A}, b = 9.18\mathring{A}, c = 5.14\mathring{A}$)

Figure 2.19: Crystal Structure of three polymorphs of TiO_2 ($\alpha = \beta = \gamma = 90°$ for all polymorphs)

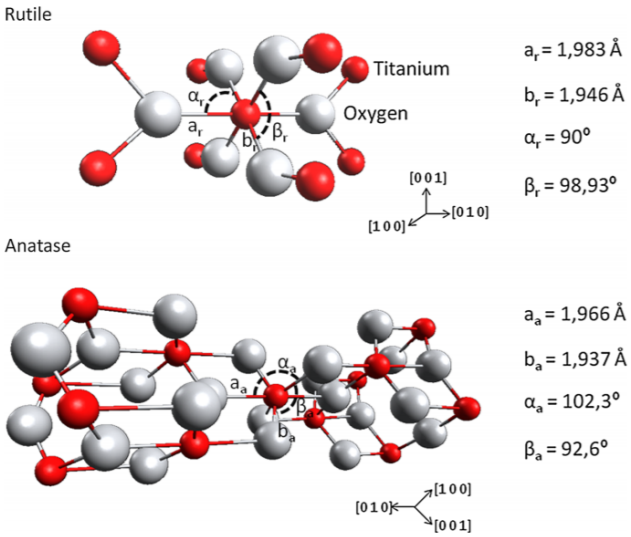

Figure 2.20: Difference in bond length and bond angles in rutile and anatase TiO_2

Cao *et al.* synthesized $Ti_{(1-x)}Sm_xO_2$ (0≤x≤0.08) via sol-gel technique [62]. Above 550°C anatase to rutile phase transition strated which became complete above 750°C. The authors have investigated the absorption spectra but they also did not characterizae the magnetic property of the samples. Shi *et al.* also investigated the photocatalytic properties of $Ti_{0.99}Sm_{0.01}O_2$ nanoparticles and observed that Sm doping suppressed the particle size. The reduction in particle size was attributed to be beneficial in photocatalytic properties of the nanoparticles [63]. Hu *et al.* studied luminiscence properties of Sm:TiO_2 nanoparticles and reported highest luminiscenece for 0.75 mol% Sm:TiO_2 nanoparticles [64]. Promising photoluminiscence and photocatalytic properties of Sm:TiO_2 were also reported in some other literatures [65–69]. None of the above mentioned research work investigated the ferromagnetic behavior of the synthesized samples. Tseng *et al.* synthesized rutile $Ti_{(1-x)}Sm_xO_2$ (0≤x≤0.02) by molten salt method and observed that dilute ferromagnetism of Sm doped TiO_2 became weaker than the ferromagnetism of undoped TiO_2 nanoparticles [70]. However, no detailed study on Sm:TiO_2 has been reported so far to the best knowledge of the author of this thesis.

CHAPTER 3

CONCLUSIONS

The objective of this thesis was to investigate the role of oxygen vacancies on ferromagnetism in TiO_2 which is one of the most promising oxide dilute magnetic semiconductors. In order to create oxygen vacancies, Ti^{4+} was substituted by Sm^{3+} in TiO_2 nanoparticles which has ∼40% larger ionic radius (109.8 pm) than Ti^{4+} (74.5 pm) ion. Due to this large variation in ionic radius, significant distortion in TiO_2 lattice is expected along with the suppression in grain growth and structural phase transition phenomena. Despite of the diffrence in ionic radius which indicates less solid solubility of Sm^{3+} in TiO_2, high concentration of Sm (20 mol%) was added to investigate the formation of second phase of dopants and their effects in structural, optical and magnetic properties of Anatase TiO_2 beyond solid solubility limit. The salient features of this thesis may be summarized as follows:

- Pristine and Sm:TiO_2 (from 0 to 20 mol% Sm) nanoparticles were synthesized by solgel method.

- X-ray diffraction analysis showed that all Bragg peaks observed in the line scans of all samples were completely matched with Anatase phase of TiO_2. Above 10 mol% of Sm substitution, a broad hump was detected in X-ray diffraction patterns which was identified as the amorphous Sm_2O_3 phase.

- The substitution of Sm was found to suppress the grain size from 53(±10) nm of pristine Anatase to 10(±3) nm of 20 mol% Sm substituted TiO_2.

- High resolution TEM images and electron diffraction study showed that no metallic clusters of Sm^{3+} ions or crystalline Sm_2O_3 were present in the samples within the detection limit.

- SAED and STEM-EDX analysis posit that the amorphous Sm_2O_3 phase might be present as atomically thin layer around the Anatase phase.

- Optical property analysis by photoluminescence and UV-Vis-NIR spectroscopy suggest that all samples exhibit indirect bandgap and the Sm incorporation reduced the bandgap from 3.0 eV of pristine Anatase to 2.47 eV of 20 mol% Sm:TiO_2 sample.

- The Sm addition increased the concentration of oxygen vacancy which create shallow trap centers just below the conduction band. The presence of these

trap centers manifests the visible photoluminescence due to the recombination of mobile electrons in the trap centers with the holes in the valence band.

- Magnetization vs. applied field characteristics show that Sm:TiO_2 samples show dilute ferromagnetism at room temperature (300 K). At 5 K temperature, an evolution of paramagnetic behavior along with ferromagnetic response was noticed in the M-H graphs of all samples.

CHAPTER 4

SUGGESTIONS FOR FUTURE WORK

- Investigation of magnetization vs. applied field characteristics at several temperatures between 5 K and 300 K in order to understand the evolution of paramagnetic response along with ferromagnetic behavior.

- Investigation of temperature vs. resistivity from 5 K to 300 K in order to observe the semiconducting behavior of the pristine and Sm:TiO_2 samples.

- Investigation of photocatalytic dye degradation by pristine and Sm:TiO_2 samples under both UV and Visible light irradiation.

- Fabrication of $Ti_{(1-x)}Sm_{(x)}O_2$ ($0 \leq x \leq 5$) thin films and study the spin polarization by X-ray Magnetic Circular Dichroism (XMCD).

Bibliography

[1] TC Kreutz, EG Gwinn, R Artzi, R Naaman, H Pizem, and CN Sukenik. Modification of ferromagnetism in semiconductors by molecular monolayers. *Applied physics letters*, 83(20):4211–4213, 2003.

[2] Supriyo Datta and Biswajit Das. Electronic analog of the electro-optic modulator. *Applied Physics Letters*, 56(7):665–667, 1990.

[3] S. Das Sarma, J. Fabian, X. Hu, and I. Zutić. Theoretical perspectives on spintronics and spin-polarized transport. *IEEE Transactions on Magnetics*, 36(5 I):2821–2826, 2000.

[4] F Matsukura, H Ohno, A Shen, and Y Sugawara. Transport properties and origin of ferromagnetism in (Ga,Mn)As. *Physical Review B*, 57(4):R2037, 1998.

[5] R. A. de Groot, F. M. Mueller, P. G. van Engen, and K. H. J. Buschow. New class of materials: Half-metallic ferromagnets. *Phys. Rev. Lett.*, 50:2024–2027, Jun 1983.

[6] JMD Coey and M Venkatesan. Half-metallic ferromagnetism: Example of cro_2. *Journal of Applied Physics*, 91(10):8345–8350, 2002.

[7] Jacek K Furdyna. Diluted magnetic semiconductors. *Journal of Applied Physics*, 64(4):R29–R64, 1988.

[8] H Munekata, H Ohno, S Von Molnar, Armin Segmüller, LL Chang, and L Esaki. Diluted magnetic iii-v semiconductors. *Physical Review Letters*, 63(17):1849, 1989.

[9] Yuji Matsumoto, Makoto Murakami, Tomoji Shono, Tetsuya Hasegawa, Tomoteru Fukumura, Masashi Kawasaki, Parhat Ahmet, Toyohiro Chikyow, Shinya Koshihara, and Hideomi Koinuma. Room-temperature ferromagnetism in transparent transition metal-doped titanium dioxide. *Science*, 291(5505):854–856, 2001.

[10] JB Yi, CC Lim, GZ Xing, HM Fan, LH Van, SL Huang, KS Yang, XL Huang, XB Qin, BY Wang, et al. Ferromagnetism in dilute magnetic semiconductors through defect engineering: Li-doped zno. *Physical review letters*, 104(13):137201, 2010.

[11] Kenji Ueda, Hitoshi Tabata, and Tomoji Kawai. Magnetic and electric properties of transition-metal-doped zno films. *Applied Physics Letters*, 79(7):988–990, 2001.

[12] SB Ogale, RJ Choudhary, JP Buban, SE Lofland, SR Shinde, SN Kale, VN Kulkarni, J Higgins, C Lanci, JR Simpson, et al. High temperature ferromagnetism with a giant magnetic moment in transparent co-doped sn$o_{2-\delta}$. *Physical Review Letters*, 91(7):077205, 2003.

[13] John Philip, Nikoleta Theodoropoulou, Geetha Berera, Jagadeesh S Moodera, and Biswarup Satpati. High-temperature ferromagnetism in manganese-doped indium-tin oxide films. *Applied Physics Letters*, 85(5):777–779, 2004.

[14] A Sundaresan, R Bhargavi, N Rangarajan, U Siddesh, and CNR Rao. Ferromagnetism as a universal feature of nanoparticles of the otherwise nonmagnetic oxides. *Physical Review B*, 74(16):161306, 2006.

[15] Nguyen Hoa Hong, Joe Sakai, Nathalie Poirot, and Virginie Brizé. Room-temperature ferromagnetism observed in undoped semiconducting and insulating oxide thin films. *Physical Review B*, 73(13):132404, 2006.

[16] M Venkatesan, CB Fitzgerald, and JMD Coey. Thin films: unexpected magnetism in a dielectric oxide. *Nature*, 430(7000):630, 2004.

[17] James L Erskine and EA Stern. Calculation of the m 23 magneto-optical absorption spectrum of ferromagnetic nickel. *Physical Review B*, 12(11):5016, 1975.

[18] Gerrit van der Laan, Bernard T Thole, George A Sawatzky, Jeroen B Goedkoop, John C Fuggle, Jean-Marc Esteva, Ramesh Karnatak, JP Remeika, and Hanna A Dabkowska. Experimental proof of magnetic x-ray dichroism. *Physical Review B*, 34(9):6529, 1986.

[19] Fabrice Wilhelm. Magnetic materials probed with polarized x-ray spectroscopies, 2013.

[20] Gerrit van der Laan and Adriana I Figueroa. X-ray magnetic circular dichroism—a versatile tool to study magnetism. *Coordination Chemistry Reviews*, 277:95–129, 2014.

[21] T Hayashi, M Tanaka, T Nishinaga, and H Shimada. Magnetic and magnetotransport properties of new iii-v diluted magnetic semiconductors: Gamnas. *Journal of applied physics*, 81(8):4865–4867, 1997.

[22] H Ohldag, V Solinus, FU Hillebrecht, JB Goedkoop, Marco Finazzi, F Matsukura, and H Ohno. Magnetic moment of mn in the ferromagnetic semiconductor (ga 0.98 mn 0.02) as. *Applied Physics Letters*, 76(20):2928–2930, 2000.

[23] M Khalid, Eugen Weschke, W Skorupa, M Helm, and Shengqiang Zhou. Ferromagnetism and impurity band in a magnetic semiconductor: Inmnp. *Physical Review B*, 89(12):121301, 2014.

[24] MA Scarpulla, BL Cardozo, R Farshchi, WM Hlaing Oo, MD McCluskey, KM Yu, and OD Dubon. Ferromagnetism in $ga_{(1-x)}mn_xp$: evidence for inter-mn exchange mediated by localized holes within a detached impurity band. *Physical review letters*, 95(20):207204, 2005.

[25] AX Gray, Jan Minar, S Ueda, PR Stone, Y Yamashita, J Fujii, J Braun, L Plucinski, CM Schneider, G Panaccione, et al. Bulk electronic structure of the dilute magnetic semiconductor $ga_{(1-x)}mn_xas$ through hard x-ray angle-resolved photoemission. *Nature materials*, 11(11):957, 2012.

[26] Masaki Kobayashi, Iriya Muneta, Yukiharu Takeda, Yoshihisa Harada, Atsushi Fujimori, Juraj Krempaskỳ, Thorsten Schmitt, Shinobu Ohya, Masaaki Tanaka, Masaharu Oshima, et al. Unveiling the impurity band induced ferromagnetism in the magnetic semiconductor (ga, mn) as. *Physical Review B*, 89(20):205204, 2014.

[27] Slavomír Nemšák, Mathias Gehlmann, Cheng-Tai Kuo, Shih-Chieh Lin, Christoph Schlueter, Ewa Mlynczak, Tien-Lin Lee, Lukasz Plucinski, Hubert Ebert, Igor Di Marco, et al. Element-and momentum-resolved electronic structure of the dilute magnetic semiconductor manganese doped gallium arsenide. *Nature communications*, 9(1):3306, 2018.

[28] Armela Keqi, Mathias Gehlmann, Giuseppina Conti, Slavomír Nemšák, Arunothai Rattanachata, Jan Minár, L Plucinski, Julien E Rault, Jean Pascal Rueff, M Scarpulla, et al. Electronic structure of the dilute magnetic semiconductor $ga_{(1-x)}mn_xp$ from hard x-ray photoelectron spectroscopy and angle-resolved photoemission. *Physical Review B*, 97(15):155149, 2018.

[29] Lijuan Zhao, Bei Zhang, Qi Pang, Shihe Yang, Xixiang Zhang, Weikun Ge, and Jiannong Wang. Chemical synthesis and magnetic properties of dilute magnetic znte: Cr crystals. *Applied physics letters*, 89(9):092111, 2006.

[30] A Haury, A Wasiela, A Arnoult, J Cibert, S Tatarenko, T Dietl, and Y Merle d'Aubigné. Observation of a ferromagnetic transition induced by two-dimensional hole gas in modulation-doped cdmnte quantum wells. *Physical Review Letters*, 79(3):511, 1997.

[31] Kesong Yang, Rongqin Wu, Lei Shen, Yuan Ping Feng, Ying Dai, and Baibiao Huang. Origin of d 0 magnetism in ii-vi and iii-v semiconductors by substitutional doping at anion site. *Physical Review B*, 81(12):125211, 2010.

[32] Tomasz Dietl. A ten-year perspective on dilute magnetic semiconductors and oxides. *Nature materials*, 9(12):965, 2010.

[33] JMD Coey, M Venkatesan, and CB Fitzgerald. Donor impurity band exchange in dilute ferromagnetic oxides. *Nature materials*, 4(2):173, 2005.

[34] J Philip, A Punnoose, BI Kim, KM Reddy, S Layne, JO Holmes, B Satpati, PR Leclair, TS Santos, and JS Moodera. Carrier-controlled ferromagnetism in transparent oxide semiconductors. *Nature materials*, 5(4):298, 2006.

[35] JMD Coey. High-temperature ferromagnetism in dilute magnetic oxides. *Journal of applied physics*, 97(10):10D313, 2005.

[36] Tomasz Dietl. Origin and control of ferromagnetism in dilute magnetic semiconductors and oxides. *Journal of Applied Physics*, 103(7):07D111, 2008.

[37] JMD Coey and SA Chambers. Oxide dilute magnetic semiconductors—fact or fiction? *MRS bulletin*, 33(11):1053–1058, 2008.

[38] Y Yamada, K Ueno, T Fukumura, HT Yuan, H Shimotani, Y Iwasa, L Gu, S Tsukimoto, Y Ikuhara, and M Kawasaki. Electrically induced ferromagnetism at room temperature in cobalt-doped titanium dioxide. *Science*, 332(6033):1065–1067, 2011.

[39] H Saadaoui, X Luo, Z Salman, XY Cui, NN Bao, P Bao, RK Zheng, LT Tseng, YH Du, T Prokscha, et al. Intrinsic ferromagnetism in the diluted magnetic semiconductor co:tio 2. *Physical review letters*, 117(22):227202, 2016.

[40] Zhihu Sun, Wensheng Yan, Guobin Zhang, Hiroyuki Oyanagi, Ziyu Wu, Qinghua Liu, Wenqing Wu, Tongfei Shi, Zhiyun Pan, Pengshou Xu, et al. Evidence of substitutional co ion clusters in zn 1- x co x o dilute magnetic semiconductors. *Physical Review B*, 77(24):245208, 2008.

[41] N Sai Krishna, S Kaleemulla, G Amarendra, N Madhusudhana Rao, C Krishnamoorthi, M Kuppan, M Rigana Begam, D Sreekantha Reddy, and I Omkaram. Structural, optical, and magnetic properties of fe doped in2o3 powders. *Materials Research Bulletin*, 61:486–491, 2015.

[42] Eva Pellicer, Enric Menendez, Jordina Fornell, Josep Nogues, Andre Vantomme, Kristiaan Temst, and Jordi Sort. Mesoporous oxide-diluted magnetic semiconductors prepared by co implantation in nanocast 3d-ordered in_2o_{3-y} materials. *The Journal of Physical Chemistry C*, 117(33):17084–17091, 2013.

[43] Shokouh S Farvid, Manu Hegde, and Pavle V Radovanovic. Influence of the host lattice electronic structure on dilute magnetic interactions in polymorphic cr (iii)-doped in2o3 nanocrystals. *Chemistry of Materials*, 25(2):233–244, 2013.

[44] Kuang Hong Gao, Zhi Qing Li, Tao Du, En Yong Jiang, and Yang Xian Li. Ferromagnetic properties of bulk $cu_{(1-x)}mn_xo$ magnetic semiconductors. *Physical Review B*, 75(17):174444, 2007.

[45] A Thurber, KM Reddy, V Shutthanandan, Mark H Engelhard, C Wang, Jason Hays, and Alex Punnoose. Ferromagnetism in chemically synthesized ceo_2 nanoparticles by ni doping. *Physical Review B*, 76(16):165206, 2007.

[46] Vinod K Paidi, Dale L Brewe, John W Freeland, Charles A Roberts, and Johan van Lierop. Role of ce 4 f hybridization in the origin of magnetism in nanoceria. *Physical Review B*, 99(18):180403, 2019.

[47] T Ohtsuki, A Chainani, Ritsuko Eguchi, M Matsunami, Y Takata, M Taguchi, Y Nishino, K Tamasaku, M Yabashi, T Ishikawa, et al. role of ti 3d carriers in mediating the ferromagnetism of co:tio2 anatase thin films. *Physical review letters*, 106(4):047602, 2011.

[48] Tiffany C Kaspar, T Droubay, V Shutthanandan, Steve M Heald, Chong M Wang, David E McCready, Suntharampillai Thevuthasan, JD Bryan, Daniel R Gamelin, AJ Kellock, et al. Ferromagnetism and structure of epitaxial cr-doped anatase tio 2 thin films. *Physical Review B*, 73(15):155327, 2006.

[49] Talita E de Souza, Alexandre Mesquita, Angela O de Zevallos, Fanny Beron, Kleber R Pirota, Person P Neves, Antonio C Doriguetto, and Hugo B de Carvalho. Structural and magnetic properties of dilute magnetic oxide based on nanostructured co-doped anatase tio2 ($ti_{(1-x)}co_xo_{2-\delta}$). *The Journal of Physical Chemistry C*, 117(25):13252–13260, 2013.

[50] Md Abdullah Al Mamun, Manifa Noor, AKM Atique Ullah, Md Sarowar Hossain, Matin Abdul, Fakhrul Islam, and MA Hakim. Effect of cepo4 on structural, magnetic and optical properties of ceria nanoparticles. *Materials Research Express*, 6(1):016102, 2018.

[51] J Daniel Bryan, Steven A Santangelo, Sean C Keveren, and Daniel R Gamelin. Activation of high-tc ferromagnetism in co2+: Tio2 and cr3+: Tio2 nanorods and nanocrystals by grain boundary defects. *Journal of the American Chemical Society*, 127(44):15568–15574, 2005.

[52] Biswajit Choudhury and Amarjyoti Choudhury. Oxygen vacancy and dopant concentration dependent magnetic properties of mn doped tio2 nanoparticle. *Current Applied Physics*, 13(6):1025–1031, 2013.

[53] Batakrushna Santara, PK Giri, Soumen Dhara, Kenji Imakita, and Minoru Fujii. Oxygen vacancy-mediated enhanced ferromagnetism in undoped and fe-doped tio2 nanoribbons. *Journal of Physics D: Applied Physics*, 47(23):235304, 2014.

[54] Shih-Yun Chen, Yi-Hsing Lu, Tzu-Wen Huang, Der-Chung Yan, and Chung-Li Dong. Oxygen vacancy dependent magnetism of ceo2 nanoparticles prepared by thermal decomposition method. *The Journal of Physical Chemistry C*, 114(46):19576–19581, 2010.

[55] GS Chang, J Forrest, EZ Kurmaev, AN Morozovska, MD Glinchuk, JA McLeod, A Moewes, TP Surkova, and Nguyen Hoa Hong. Oxygen-vacancy-induced ferromagnetism in undoped sno_2 thin films. *Physical Review B*, 85(16):165319, 2012.

[56] Hyeon-Jun Lee, Se-Young Jeong, Chae Ryong Cho, and Chul Hong Park. Study of diluted magnetic semiconductor: Co-doped zno. *Applied Physics Letters*, 81(21):4020–4022, 2002.

[57] Nguyen Hoa Hong, Joe Sakai, Ngo Thu Huong, Nathalie Poirot, and Antoine Ruyter. Role of defects in tuning ferromagnetism in diluted magnetic oxide thin films. *Physical Review B*, 72(4):045336, 2005.

[58] V Fernandes, RJO Mossanek, P Schio, JJ Klein, AJA De Oliveira, WA Ortiz, N Mattoso, J Varalda, WH Schreiner, M Abbate, et al. Dilute-defect magnetism: Origin of magnetism in nanocrystalline ceo 2. *Physical Review B*, 80(3):035202, 2009.

[59] NV Skorodumova, SI Simak, Bengt I Lundqvist, IA Abrikosov, and Börje Johansson. Quantum origin of the oxygen storage capability of ceria. *Physical Review Letters*, 89(16):166601, 2002.

[60] Norifusa Satoh, Toshio Nakashima, and Kimihisa Yamamoto. Metastability of anatase: size dependent and irreversible anatase-rutile phase transition in atomic-level precise titania. *Scientific reports*, 3:1959, 2013.

[61] Qi Xiao, Zhichun Si, Zhiming Yu, and Guanzhou Qiu. Sol–gel auto-combustion synthesis of samarium-doped tio2 nanoparticles and their photocatalytic activity under visible light irradiation. *Materials Science and Engineering: B*, 137(1-3):189–194, 2007.

[62] Yuechan Cao, Zongyan Zhao, Juan Yi, Chenshuo Ma, Dacheng Zhou, Rongfei Wang, Chen Li, and Jianbei Qiu. Luminescence properties of sm3+-doped tio2 nanoparticles: Synthesis, characterization, and mechanism. *Journal of Alloys and Compounds*, 554:12–20, 2013.

[63] Jianwen Shi, Jingtang Zheng, Yan Hu, and Yucui Zhao. Photocatalytic degradation of methyl orange in water by samarium-doped tio2. *Environmental Engineering Science*, 25(4):489–496, 2008.

[64] Lanying Hu, Hongwei Song, Guohui Pan, Bin Yan, Ruifei Qin, Qilin Dai, Libo Fan, Suwen Li, and Xue Bai. Photoluminescence properties of samarium-doped tio2 semiconductor nanocrystalline powders. *Journal of Luminescence*, 127(2):371–376, 2007.

[65] V Kiisk, I Sildos, S Lange, V Reedo, T Tätte, M Kirm, and J Aarik. Photoluminescence characterization of pure and sm3+-doped thin metaloxide films. *Applied Surface Science*, 247(1-4):412–417, 2005.

[66] Dong Jin Park, Tohru Sekino, Satoshi Tsukuda, Asuka Hayashi, Takafumi Kusunose, and Shun-Ichiro Tanaka. Photoluminescence of samarium-doped tio2 nanotubes. *Journal of Solid State Chemistry*, 184(10):2695–2700, 2011.

[67] V Aware Dinkar, S Jadhav Shridhar, E Navgire Madhukar, E Athare Anil, and H Kolhe Nitin. Sm-doped tio2 nanoparticles with high photocatalytic activity for ars dye under visible light synthesized by ultrasonic assisted sol-gel method. *Oriental Journal of Chemistry*, 32(2):933–940, 2016.

[68] Yunfei Ma, Jinlong Zhang, Baozhu Tian, Feng Chen, and Lingzhi Wang. Synthesis and characterization of thermally stable sm, n co-doped tio2 with highly visible light activity. *Journal of Hazardous Materials*, 182(1-3):386–393, 2010.

[69] Yan Xiang, Zhu Ma, Jia Zhuang, Honglin Lu, Chunyang Jia, Junsheng Luo, Haimin Li, and Xiaowei Cheng. Enhanced performance for planar perovskite solar cells with samarium-doped tio2 compact electron transport layers. *The Journal of Physical Chemistry C*, 121(37):20150–20157, 2017.

[70] Li-Ting Tseng, Xi Luo, Sean Li, and Jiabao Yi. Magnetic properties of sm-doped rutile tio2 nanorods. *Journal of Alloys and Compounds*, 687:294–299, 2016.